

Ionic Hydrogen Bonds in Bioenergetics. 4. Interaction Energies of Acetylcholine with Aromatic and Polar Molecules

Carol A. Deakne*[‡] and Michael Meot-Ner (Mautner)*[†]

Contribution from the Department of Chemistry, Eastern Illinois University, Charleston, Illinois 61920, and Chemical Kinetics and Thermodynamics Division, National Institute of Standards and Technology, Gaithersburg, Maryland 20899

Received July 20, 1998

Abstract: The binding energies of the quaternary ions $(\text{CH}_3)_4\text{N}^+$ and acetylcholine (ACh) to neutral molecules have been measured by pulsed high-pressure mass spectrometry and calculated ab initio, to model interactions in the acetylcholine receptor channel. Binding energies to C_6H_6 and $\text{C}_6\text{H}_5\text{CH}_3$ are similar to those to H_2O (33–42 kJ/mol (8–10 kcal/mol)), but are weaker than those to polar organic ligands such as $\text{CH}_3\text{CO}_2\text{CH}_3$ (50–63 kJ/mol (12–15 kcal/mol)) and to amides (up to 84 kJ/mol (20 kcal/mol)). These data suggest that aromatic residues that line the groove leading to the ACh receptor site may provide stabilization comparable to water, and therefore allow entry from the aqueous environment, yet do not bind ACh as strongly as polar protein groups, and therefore allow transit, without trapping, to the receptor site. Four of the five distinct ACh conformers located computationally are stabilized by internal $\text{C}-\text{H}\cdots\text{O}$ hydrogen bonds involving the quaternary ammonium group, which is supported by the thermochemistry of the protonated analogue, $\text{CH}_3\text{CO}_2\text{CH}_2\text{CH}_2\text{N}-(\text{CH}_3)_2\text{H}^+$, and by the measured bonding energy between models of the ACh end groups, $(\text{CH}_3)_4\text{N}^+$ and $\text{CH}_3\text{-CO}_2\text{CH}_3$. Each conformer forms a number of stable complexes with water or benzene. Several possible roles for an ACh conformational change upon entry into the channel are discussed, including partial compensation for the loss of bulk solvation. An additional role for the aromatic environment is also suggested, namely lowering the energy barrier to the formation of the active all-trans ACh rotamer required at the receptor site.

Introduction

Recent studies^{1–3} have shown that the neurotransmitter acetylcholine (ACh, $\text{CH}_3\text{CO}_2\text{CH}_2\text{CH}_2\text{N}(\text{CH}_3)_3^+$) traverses a deep groove lined with aromatic amino acids after leaving the aqueous environment of the synaptic cleft and before reaching the active site in acetylcholinesterase (AChE). Together with three water molecules, some of these aromatic residues also bind to the choline end of ACh in the active site. The ACh transport process is similar to the transit of K^+ through potassium channels, where the ion binds to aromatic residues. It has been suggested that these ion–aromatic interactions (more generally termed cation– π interactions) assist in desolvating K^+ and provide ion selectivity.^{4–6} We have argued qualitatively that the aromatic residues in the ACh receptor channel may assist similarly in desolvation, while providing a weakly bonding environment that does not trap ACh but allows its transit to the more strongly bonding receptor site.⁷ We also have made a qualitative suggestion that intramolecular solvation in ACh itself,

between the quaternary ionic group and the acetyl group, may help in the desolvation process.

Both unconventional and conventional hydrogen bonds are involved in the intramolecular and intermolecular solvation of ACh. In contrast to the conventional $\text{O}-\text{H}\cdots\text{O}$ interactions, there is unlikely to be a significant amount of n-donation into the bond in the unconventional $\text{C}-\text{H}\cdots\text{O}$ and $\text{C}-\text{H}\cdots\pi$ interactions. In the latter cases the term hydrogen bonding indicates only that polar and/or polarizable ligands interact with partially charged hydrogen atoms.^{6,8–12} In addition to their role in substrate/ligand binding and ion selectivity, unconventional interactions have been invoked to account for crystal packing motifs and observed conformational preferences.^{6,13,14}

The strengths of the interactions between an ion such as ACh and surrounding solvent molecules are important in computational modeling, but cannot be obtained directly in the complex biological environment. However, these forces can be measured in isolated gas-phase clusters. For example, we constructed a cluster model of the active site of serine proteases, which suggested substantial assistance by surrounding peptide amide

[‡] Eastern Illinois University.

[†] National Institute of Standards and Technology. Current address: Department of Chemistry, University of Canterbury, Christchurch 8001, New Zealand.

(1) Sussman, J. L.; Harel, M.; Frolow, F.; Oefner, C.; Goldman, A.; Toker, L.; Silman, I. *Science* **1991**, *253*, 871–879.

(2) Sussman, J. L.; Silman, I. *Curr. Opin. Struct. Biol.* **1992**, *2*, 721–729.

(3) Harel, M.; Quinn, D. M.; Nair, H. K.; Silman, I.; Sussman, J. L. *J. Am. Chem. Soc.* **1996**, *118*, 2340–2346.

(4) Dougherty, D. A.; Stauffer, D. A. *Science* **1990**, *250*, 1558–1560.

(5) Kumpf, R. A.; Dougherty, D. A. *Science* **1993**, *261*, 1708–1710.

(6) Dougherty, D. A. *Science* **1996**, *271*, 163–168.

(7) Meot-Ner (Mautner), M. In *Computational Approaches in Supramolecular Chemistry*; Wipff, G., Ed.; Kluwer Academic: Dordrecht, 1994; NATO ASI Series C, Vol. 426, pp 31–49.

(8) Taylor, R.; Kennard, O. *Acc. Chem. Res.* **1984**, *17*, 320–326.

(9) Meot-Ner (Mautner), M.; Deakne, C. A. *J. Am. Chem. Soc.* **1985**, *107*, 469–474.

(10) Steiner, T.; Saenger, W. *J. Am. Chem. Soc.* **1992**, *114*, 10146–10154.

(11) Aakeröy, C. B.; Sneddon, K. R. *Chem. Soc. Rev.* **1993**, *22*, 397–407.

(12) Lee, J. Y.; Lee, S. J.; Choi, H. S.; Cho, S. J.; Kim, K. S.; Ha, T.-K. *Chem. Phys. Lett.* **1995**, *232*, 67–71.

(13) Viswamitra, M. A.; Radhakrishnan, R.; Bandekar, J.; Desiraju, G. R. *J. Am. Chem. Soc.* **1993**, *115*, 4868–4869.

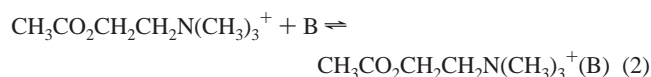
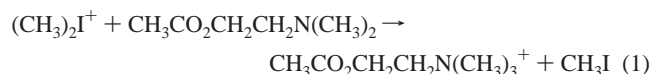
(14) Gil, F. P. S. C.; Amorim da Costa, A. M.; Teixeira-Dias, J. J. C. *J. Phys. Chem.* **1995**, *99*, 8066–8070.

groups.¹⁵ Both experiments^{9,16,17} and ab initio computations^{9,12,17–21} indicate that the binding energies of the ammonium ion NH_4^+ and of the tetramethylammonium ion $(\text{CH}_3)_4\text{N}^+$ with water are approximately equal to their binding energies with benzene and toluene. The NH_4^+ –4-methylindole and $(\text{CH}_3)_4\text{N}^+$ –4-methylindole interaction energies are 17–29 kJ/mol (4–7 kcal/mol) stronger than those with H_2O .²¹ These data suggest that interactions between ACh and aromatic groups could be competitive in stability with those between ACh and water. However, these studies have taken into account neither the possible effect of interactions with the acetoxy end of ACh on the relative binding energies nor the possible effect of a change in the conformation of ACh on the relative binding energies.

In this paper we present a combined experimental and computational study of cluster models of interactions related to ACh entry into the enzyme groove and to ACh binding in the active site. Although the measurements are limited by experimental constraints, they provide data that can help to calibrate the theoretical calculations, and the combined study provides hints about the relationship between structure and function in the ACh system. Fuxreiter and Warshel have also modeled the binding of ACh to polar and nonpolar residues, but they concentrated on the catalysis of the acylation reaction.²²

Experimental and Computational Details

The measurements were performed with the NIST pulsed high-pressure mass spectrometer and equilibrium methods as described previously.²³ In essence, the method consists of generating ACh in the gas phase by methylation of the amine precursor $\text{CH}_3\text{CO}_2\text{CH}_2\text{CH}_2\text{N}(\text{CH}_3)_2$ in reaction 1 and observing the clustering equilibrium of ACh with solvent or ligand molecules B in reaction 2. Specifically, clustering equilibria with H_2O , $(\text{CH}_3)_2\text{CO}$, 3- $\text{CH}_3\text{C}_6\text{H}_4\text{OH}$, $\text{C}_6\text{H}_5\text{OCH}_3$, and $\text{C}_6\text{H}_5\text{-CH}_3$ were investigated. When possible the temperature dependence of K_2 was measured to obtain ΔH°_2 and ΔS°_2 .



For similar studies on $(\text{CH}_3)_4\text{N}^+$, the tetramethylammonium ions were produced by CH_3^+ transfer from $(\text{CH}_3)_2\text{Cl}^+$ to $(\text{CH}_3)_3\text{N}$. $(\text{CH}_3)_4\text{N}^+$ was generated by fast reactions following the ionization of a mixture of 3–5 mbar of N_2 carrier gas, 0.002 mbar of CH_3Cl , and approximately 0.0002 mbar of $(\text{CH}_3)_3\text{N}$. ACh, $\text{CH}_3\text{CO}_2\text{CH}_2\text{CH}_2\text{N}(\text{CH}_3)_3^+$, was generated from mixtures containing 2–4 mbar of N_2 carrier gas, about 0.1 mbar of CH_3Cl , about 0.01 mbar of CH_3I , and 0.0001 mbar of $\text{CH}_3\text{-CO}_2\text{CH}_2\text{CH}_2\text{N}(\text{CH}_3)_2$. In this case $(\text{CH}_3)_2\text{I}^+$ is produced by a rapid sequence of CH_3^+ transfer reactions, which are followed by reaction 1 to yield the ACh ion. ACh is the stable product since its neutral precursor has the highest methyl cation affinity in the system. In the clustering studies 0.0001–0.001 mbar of the vaporized ligand was also added. For the $(\text{CH}_3)_4\text{N}^+$ complexes, $\text{B} = \text{CH}_3\text{CO}_2\text{CH}_3$ and C_6H_6 .

(15) Meot-Ner (Mautner), M. *J. Am. Chem. Soc.* **1988**, *110*, 3071–3075.

(16) Meot-Ner (Mautner), M. *J. Am. Chem. Soc.* **1984**, *106*, 1265–1272.

(17) Deakyne, C. A.; Meot-Mer (Mautner), M. *J. Am. Chem. Soc.* **1985**, *107*, 474–479.

(18) Deakyne, C. A. *J. Phys. Chem.* **1986**, *90*, 6625–6632.

(19) Deakyne, C. A. *Mol. Struct. Energ.* **1987**, *4*, 105–141.

(20) Kim, K. S.; Lee, J. Y.; Lee, S. J.; Ha, T.-K.; Kim, D. H. *J. Am. Chem. Soc.* **1994**, *116*, 7399–7400.

(21) Basch, H.; Stevens, W. J. *J. Mol. Struct. (THEOCHEM)* **1995**, *338*, 303–315.

(22) Fuxreiter, M.; Warshel, A. *J. Am. Chem. Soc.* **1998**, *120*, 183–194.

(23) Meot-Ner (Mautner), M.; Sieck, L. W. *J. Am. Chem. Soc.* **1991**, *113*, 4448–4460.

A possible isomeric product may be formed in reaction 1 by alkylation of the ester group. The CH_3I reactant was added to generate $(\text{CH}_3)_2\text{I}^+$ as the dimethylhalonium ion, from which CH_3^+ transfer will be least exothermic and therefore the most energetically selective. This procedure should help to methylate the amine group selectively, since the methyl cation affinity of the dimethylamino group is expected to be substantially higher than that of the ester group, in parallel with the relative proton affinities of esters and amines. Also, we have observed that methylated acetone transfers CH_3^+ rapidly to $\text{CH}_3\text{CO}_2\text{CH}_2\text{CH}_2\text{N}(\text{CH}_3)_2$. Analogously, intramolecular CH_3^+ transfer from the ester to the amino group may be fast, even if the oxygen-methylated ion is generated first. For these reasons, we consider that the observed species is indeed the quaternary ACh ion.

For the proton affinity measurements, CH_4 was used as the carrier gas at 3.2–6.4 mbar. The mixture also contained 0.0002–0.0005 mbar of $(\text{CH}_3)_3\text{N}$ and 0.0001–0.001 mbar of $\text{CH}_3\text{CO}_2\text{CH}_2\text{CH}_2\text{N}(\text{CH}_3)_2$.

In all cases the reactants were mixed in a 3 L glass bulb at 150 °C and introduced into the ion source through stainless steel lines heated to 150 °C. The reactant mixtures were ionized by 1 ms pulses of 1000–2000 eV electrons. Ion intensities issuing from the ion source were observed to 2–4 ms reaction times after the end of the ionizing pulse.

Fully optimized structures of ACh, $\text{ACh}(\text{H}_2\text{O})$, $\text{ACh}(\text{H}_2\text{O})_2$, $\text{ACh}(\text{C}_6\text{H}_6)$, and $\text{ACh}(\text{C}_6\text{H}_6)_2$ were computed ab initio with the Gaussian 94 series of programs²⁴ on a Cray X-MP computer. Bond lengths have been optimized to 0.001 Å and bond angles to 0.1°. Since the complexes have as many as 22 heavy atoms, the optimizations have been carried out at the HF/6-31G(d) level of calculation. This calculational level has been used extensively to obtain geometries of hydrogen-bonded complexes and is generally reliable.^{25–28} There have been cases reported for which the potential energy surface contains two minima at the HF level and one minimum at the correlated level.^{28–30} Possible hydrogen-bonded interactions in the $\text{ACh}(\text{H}_2\text{O})_n$ and $\text{ACh}(\text{C}_6\text{H}_6)_n$ complexes are $\text{O}-\text{H}\cdots\text{O}=\text{C}$, $\text{O}-\text{H}\cdots\text{O}-\text{C}$, $\text{O}-\text{H}\cdots\text{O}-\text{H}$, $\text{C}-\text{H}\cdots\text{O}=\text{C}$, $\text{C}-\text{H}\cdots\text{O}-\text{C}$, $\text{C}-\text{H}\cdots\text{O}-\text{H}$, and $\text{C}-\text{H}\cdots\pi$. Double-well proton-transfer potentials are not likely for these interactions, so the HF/6-31G(d) geometries are expected to be reliable.

A large number of equilibrium structures have been located and characterized as minima by harmonic normal-mode analysis. The HF/6-31G(d) potential energy surfaces of all of these ions are extremely shallow, and other than starting with geometries far removed from the equilibrium geometries, we have not attempted to identify either the global minimum or other local minima. However, it should be noted that several different starting configurations led to the more stable complexes. The results suggest that the conclusions obtained from this work would not be altered by locating additional minima. Moreover, since some of the trends in stability change when energies are converted to enthalpies and, especially, to free energies (see below), the idea of an “optimal structure” may have little meaning for these ions.

MP2/6-31G(d)//HF/6-31G(d) single-point energies were computed for each local minimum, since Kim and co-workers^{12,20} and Pullman and co-workers³¹ have found that electron correlation makes an important contribution to the binding of benzene and $(\text{CH}_3)_4\text{N}^+$. The

(24) Frisch, M. J.; Trucks, G. W.; Schlegel, H. B.; Gill, P. M. W.; Johnson, B. G.; Robb, M. A.; Cheeseman, J. R.; Keith, T.; Petersson, G. A.; Montgomery, J. A.; Raghavachari, K.; Al-Laham, M. A.; Zakrzewski, V. G.; Ortiz, J. V.; Foresman, J. B.; Cioslowski, J.; Stefanov, B. B.; Nanayakkara, A.; Challacombe, M.; Peng, C. Y.; Ayala, P. Y.; Chen, W.; Wong, M. W.; Andres, J. L.; Replogle, E. S.; Gomperts, R.; Martin, R. L.; Fox, D. J.; Binkley, J. S.; Defrees, D. J.; Baker, J.; Stewart, J. P.; Head-Gordon, M.; Gonzalez, C.; Pople, J. A. Gaussian 94, Revision C.3, NIST, 1995; Gaussian, Inc.: Pittsburgh, PA. Use of this program does not indicate NIST endorsement of this product.

(25) Tsuzuki, S.; Uchimaru, T.; Tanabe, K.; Hirano, T. *J. Phys. Chem.* **1993**, *97*, 1346–1350.

(26) Alemán, C.; Navas, J. J.; Muñoz-Guerra, S. *J. Phys. Chem.* **1995**, *99*, 17653–17661.

(27) Watanabe, H.; Iwata, S. *J. Phys. Chem.* **1996**, *100*, 3377–3386.

(28) Meot-Ner (Mautner), M.; Sieck, L. W.; Koretke, K. K.; Deakyne, C. A. *J. Am. Chem. Soc.* **1997**, *119*, 10430–10438.

(29) Del Bene, J. E. *J. Phys. Chem.* **1988**, *92*, 2874–2880.

(30) Pudziański, A. T. *J. Chem. Phys.* **1995**, *102*, 8029–8039.

(31) Pullman, A.; Berthier, G.; Savinelli, R. *J. Am. Chem. Soc.* **1998**, *120*, 8553–8554.

Table 1. Kinetics of Proton and Methyl Cation Transfer Reactions

reaction	k_f^a	k_r^a	$\Delta H^\circ{}^b$	$\Delta S^\circ{}^b$	$\Delta G^\circ{}^b$	T (K)
proton transfer						
$(\text{CH}_3\text{CH}_2)_3\text{NH}^+ + \text{CH}_3\text{CO}_2(\text{CH}_2)_2\text{N}(\text{CH}_3)_2 \rightarrow$	0.39	3.0	-8.8	-34.7	8.4	489
$\text{CH}_3\text{CO}_2(\text{CH}_2)_2\text{N}(\text{CH}_3)_2\text{H}^+ + (\text{CH}_3\text{CH}_2)_3\text{N}$	0.23	2.5			11.7	587
methyl cation transfer						
$(\text{CH}_3)_2\text{I}^+ + (\text{CH}_3)_2\text{CO} \rightarrow (\text{CH}_3)_2\text{COCH}_3^+ + \text{CH}_3\text{I}$	4.5					307
$(\text{CH}_3)_2\text{I}^+ + \text{CH}_3\text{CO}_2(\text{CH}_2)_2\text{N}(\text{CH}_3)_2 \rightarrow$	6.2					299
$\text{CH}_3\text{CO}_2(\text{CH}_2)_2\text{N}(\text{CH}_3)_3^+ + \text{CH}_3\text{I}$						
$(\text{CH}_3)_3\text{S}^+ + (\text{CH}_3)_3\text{N} \rightarrow (\text{CH}_3)_4\text{N}^+ + (\text{CH}_3)_2\text{S}$	<0.04					325

^a Units of $10^{-10} \text{ cm}^3 \text{ s}^{-1}$. Uncertainty estimate, based on standard deviations of replicate measurements, multiplied by a conventional coverage factor of 2, is $\pm 30\%$. Other components of the uncertainty, in particular partial pressures of the reactants, have smaller associated errors of about $\pm 10\%$. ^b ΔH° and ΔG° in kJ/mol, ΔS° in J/(mol·K). Uncertainty estimates from standard deviation of van't Hoff plot multiplied by a conventional coverage factor of 2: $\Delta H^\circ = \pm 0.8 \text{ kJ/mol}$, $\Delta S^\circ = \pm 1.7 \text{ J/(mol}\cdot\text{K)}$.

MP2 energies were combined with the zero-point and thermal translational, rotational, and vibrational energies to determine enthalpies and free energies. Most of the ACh equilibrium structures have two equivalent rotamers, which was accounted for by adjusting the expression for the entropy (eq 3).

$$S = S_{\text{trans}} + S_{\text{rot}} + S_{\text{vib}} + R \ln 2 \quad (3)$$

The main focus of the calculations is to assess the relative energies of (1) the stable conformers of ACh and (2) the stable complexes each of these conformers forms with water and benzene. We tested whether scaling the vibrational frequencies and zero-point energies by the usual factors^{32,33} altered the relative enthalpies, entropies, and free energies of the ACh conformers or ACh(H₂O) complexes. As expected, we found that the relative values were affected by $<0.4 \text{ kJ/mol}$ ($<0.1 \text{ kcal/mol}$). Consequently, none of the thermochemical quantities reported in this article have been evaluated with scaled frequencies.

Theoretical enthalpies, entropies, and free energies of association have been estimated for the ACh(H₂O), ACh(H₂O)₂, ACh(C₆H₆), and ACh(C₆H₆)₂ complexes with the MP2 data. The product cluster ion with the most stable free energy was utilized in the association reaction. The reactants were then chosen so that the reactant and product ions have the same ACh conformation. Since the calculated enthalpies of reaction are estimates, they have not been corrected for basis set superposition error.

Results and Analysis of Results

A. Kinetic Observations. Before describing the thermochemistry, we summarize some kinetic observations on proton transfer and methyl cation transfer reactions. The reversible proton-transfer reaction between $\text{CH}_3\text{CO}_2\text{CH}_2\text{CH}_2\text{N}(\text{CH}_3)_2$ and $(\text{CH}_3\text{CH}_2)_3\text{NH}^+$, reaction 4 below, was measured for proton affinity determination, and approach to equilibrium yielded the kinetic data in Table 1. We note that the reverse reaction is endothermic (see below) but proceeds at about 30% reaction efficiency. This constitutes an example of the entropy-assisted kinetics we have observed with other bifunctional molecules.³⁴

The methyl cation transfer reactions from $(\text{CH}_3)_2\text{I}^+$ to $\text{CH}_3\text{CO}_2\text{CH}_2\text{CH}_2\text{N}(\text{CH}_3)_2$ and $(\text{CH}_3)_2\text{CO}$ are near the collision rates of about $10^{-9} \text{ cm}^3 \text{ s}^{-1}$. The methylated acetone ion $(\text{CH}_3)_2\text{COCH}_3^+$ also transfers CH_3^+ rapidly to this amine, just as in the fast transfer of CH_3^+ from $(\text{CH}_3)_3\text{O}^+$ to $(\text{CH}_3)_3\text{N}$.

B. Proton Affinity and Internal Solvation. Space-filling models show that the oxygen atoms in $\text{CH}_3\text{CO}_2\text{CH}_2\text{CH}_2\text{N}(\text{CH}_3)_2$ can approach the quaternary methyl groups within the van der Waals radius. It is therefore expected that this interaction will stabilize the ion significantly in the gas phase or in desolvated environments. Unfortunately, the stability of ACh

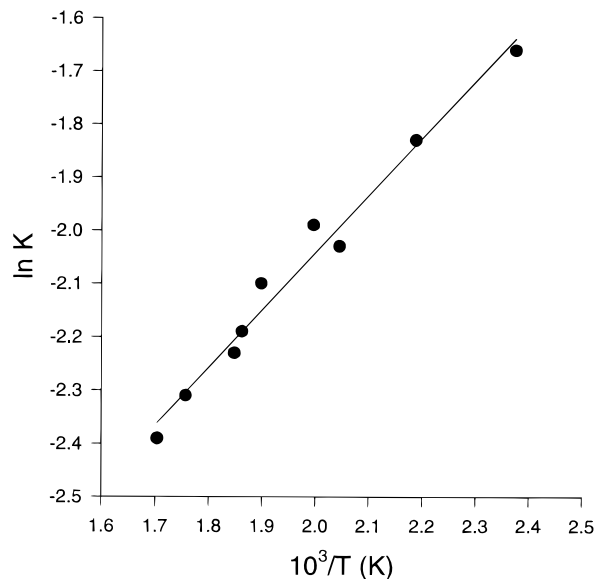
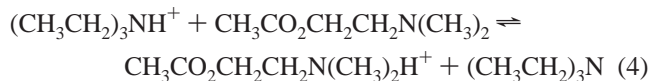


Figure 1. Van't Hoff plot for the proton-transfer reaction $(\text{CH}_3\text{CH}_2)_3\text{NH}^+ + \text{CH}_3\text{CO}_2\text{CH}_2\text{CH}_2\text{N}(\text{CH}_3)_2 \rightarrow \text{CH}_3\text{CO}_2\text{CH}_2\text{CH}_2\text{N}(\text{CH}_3)_2\text{H}^+ + (\text{CH}_3\text{CH}_2)_3\text{N}$.

cannot be measured by equilibrium methods. However, space-filling models show a similar interaction in the protonated analogue of ACh, i.e., the product ion of reaction 4. The thermochemistry of this ion can be measured by proton-transfer equilibrium to a reference base with a known proton affinity (PA). A van't Hoff plot is shown in Figure 1.



$$\Delta H^\circ = -8.8 \pm 0.8 \text{ kJ/mol}, \quad \Delta S^\circ = -34.7 \pm 1.7 \text{ J/(mol}\cdot\text{K)}$$

Without intramolecular stabilization, the PA of $\text{CH}_3\text{CO}_2\text{CH}_2\text{CH}_2\text{N}(\text{CH}_3)_2$ should be similar to that of $(\text{CH}_3)_3\text{N}$, i.e., about 948.9 kJ/mol (226.8 kcal/mol). Using $\text{PA}((\text{CH}_3\text{CH}_2)_3\text{N}) = 981.8 \text{ kJ/mol}$ (234.7 kcal/mol),³⁵ the present results yield $\text{PA}(\text{CH}_3\text{CO}_2\text{CH}_2\text{CH}_2\text{N}(\text{CH}_3)_2) = 990.6 \text{ kJ/mol}$ (236.8 kcal/mol), which is higher than that of $(\text{CH}_3)_3\text{N}$ by 41.7 kJ/mol (10.0 kcal/mol). Also, the large negative ΔS° observed for reaction 4 is similar to those observed upon formation of intramolecular hydrogen bonds in bifunctional ions.^{36,37} Therefore, the measurements suggest that intramolecular hydrogen bonding, as shown sche-

(32) Hehre, W. J.; Radom, L.; Schleyer, P. v. R.; Pople, J. A. *Ab Initio Molecular Orbital Theory*; John Wiley & Sons: New York, 1986.

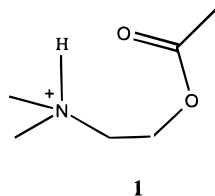
(33) Grev, R. S.; Janssen, C. L.; Schaefer, H. F., III *J. Chem. Phys.* **1991**, *95*, 5128–5132.

(34) Meot-Ner (Mautner), M. *J. Phys. Chem.* **1991**, *95*, 6580–6585.

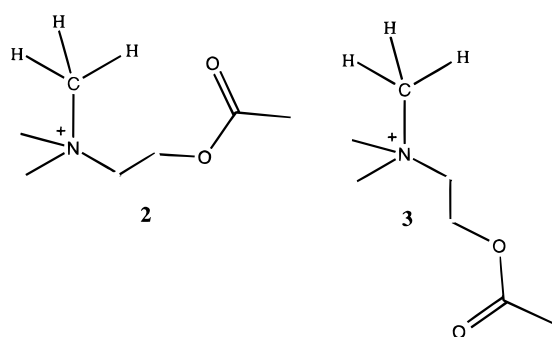
(35) Hunter, E. P.; Lias, S. G. *Proton Affinity Evaluation in NIST Chemistry WebBook*, NIST Standard Data Base Number 69; Mallard, W. G., Linstrom, P. J., Eds.; National Institute of Standards and Technology: Gaithersburg, March 1998 (<http://webbook.nist.gov>).

(36) Yamdagni, R.; Kebarle, P. *J. Am. Chem. Soc.* **1973**, *95*, 3504–3510.

matically in structure **1**, stabilizes the ion by about 40 kJ/mol (10 kcal/mol).

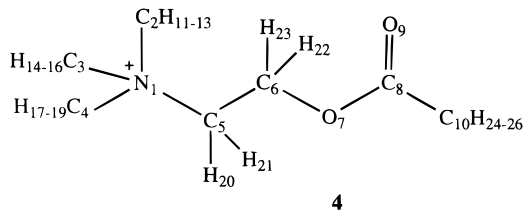


The intramolecular bonding in ACh itself, in conformation **2**, may be weaker, since hydrogen bonding to positively charged hydrogens on carbon is usually weaker than those on nitrogen. On the other hand, the internal hydrogen bond in **1** is strained and the larger size of the methyl groups allows a more optimum geometry. Thus, the internal solvation in **2** compared with the unsolvated conformation **3** may be significant.



To model this intramolecular bond between the quaternary group and the acetyl group, we measured the bond strength between $(\text{CH}_3)_4\text{N}^+$ and $\text{CH}_3\text{CO}_2\text{CH}_3$. The observed strength of 50.6 kJ/mol (12.1 kcal/mol) is substantial, and comparable to the 39 kJ/mol (9 kcal/mol) stabilizing energy observed for the protonated ion.

C. ACh Conformations. Five stable conformers of ACh have been identified in this work. The main characteristics that distinguish one conformer from another are the $\text{N}_1\text{C}_5\text{C}_6\text{O}_7$ and $\text{C}_5\text{C}_6\text{O}_7\text{C}_8$ dihedral angles. (The atomic numbering scheme is given in structure **4**.) The $\text{C}_4\text{N}_1\text{C}_5\text{C}_6$ and $\text{C}_6\text{O}_7\text{C}_8\text{C}_{10}$ dihedral angles are trans in each conformation. Each stable conformer



has been assigned a two-letter acronym labeling the $\text{N}_1\text{C}_5\text{C}_6\text{O}_7$ and $\text{C}_5\text{C}_6\text{O}_7\text{C}_8$ dihedral arrangements, in that order, as gauche (g), gauche' (g'), or trans (t). The five stable conformers of ACh are then gg', gg, gt, tg, and tt and are illustrated in Figure 2. The HF/6-31G(d) optimum geometrical parameters for each conformer are listed in Table S1 in the Supporting Information. (No such data have been included for the complexes, since there is little change in the monomer geometries when the complexes are formed. The complete set of geometrical parameters are available from the authors.)

(37) Meot-Ner (Mautner), M.; Hamlet, P.; Hunter, E. P.; Field, F. H. *J. Am. Chem. Soc.* **1980**, *102*, 6393–6399.

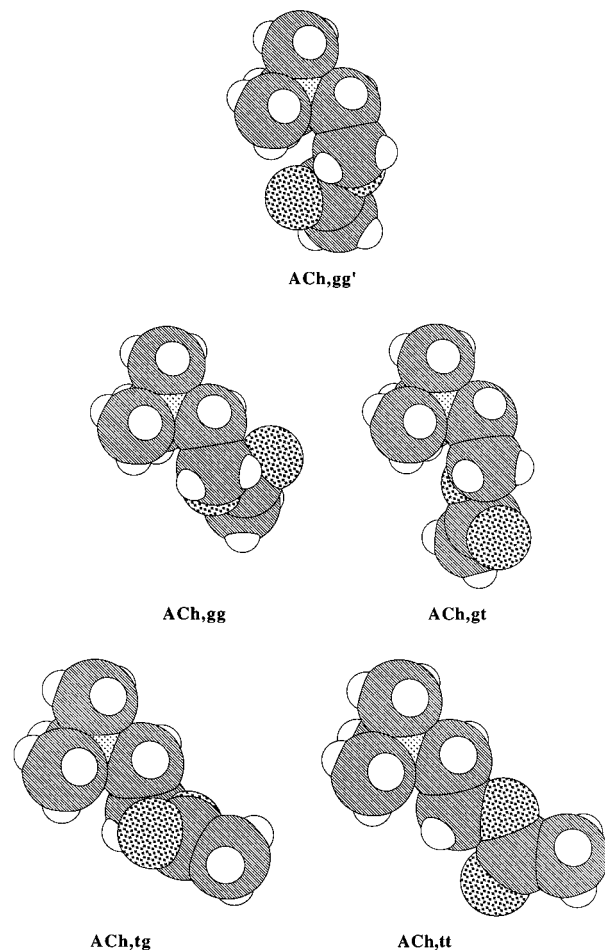


Figure 2. Space filling representations of ACh rotamers. The degrees of grayness are: C > O > N > H.

Liquori et al.³⁸ have carried out a (gas phase) conformational analysis of ACh for which the bond lengths and bond angles were held constant and the energy was calculated in terms of van der Waals pairwise interactions between nonbonded atoms and 3-fold torsional potentials. They located four of the five conformations we located, namely the gg, gt, tg, and tt conformations. Despite the flexibility of ACh expected from the gas-phase studies, solution NMR studies indicate that the gt form is preponderant in aqueous solution,³⁹ and X-ray diffraction studies indicate that the gt and gg forms are preponderant in crystals of acetylcholine salts.^{40–42} In fact for acetylcholine chloride, the cation retains the gt conformation in the crystal, in the semirigid clathrate structures of the small hydrates (up to seven water molecules), and in dilute solution.⁴³ In contrast, molecular modeling studies¹ and the X-ray structure of the *m*-(*N,N,N*-trimethylammonio)-2,2,2-trifluoroacetophenone–AChE complex suggest that ACh is in the tt conformation during the acylation stage of the catalytic mechanism.³ Clearly the conformation of ACh is influenced by the local environment.

(38) Liquori, A. M.; Damiani, A.; De Coen, J. L. *J. Mol. Biol.* **1968**, *33*, 445–450.

(39) Culvenor, C. C. J.; Ham, N. S. *Chem. Commun.* **1966**, 537–539.

(40) Svinning, T.; Sørum, H. *Acta Crystallogr., Sect. B* **1975**, *31*, 1581–1586.

(41) Jagner, S.; Jensen, B. *Acta Crystallogr., Sect. B* **1977**, *33*, 2757–2762.

(42) Datta, N.; Mondal, P.; Pauling, P. *Acta Crystallogr., Sect. B* **1980**, *36*, 906–909.

(43) Harmon, K. M.; Akin, A. C.; Avci, G. F.; Nowos, L. S.; Tierney, M. B. *J. Mol. Struct.* **1991**, *244*, 223–236.

Table 2. Selected Dihedral Angles of Acetylcholine^a

system ^b	$\angle N_1C_5C_6O_7$	$\angle C_5C_6O_7C_8$
ACh,gg' ^c	78.1	-112.6
ACh,gg ^c	67.3	78.7
ACh ^d	72.2	75.4
AChBr ^e	78.4	78.9
AChI ^f	89	83
ACh,gt ^c	62.5	171.1
ACh ^d	73.6	-178.0
AChTPB ^g	66.7	154.6
AChCl ^h	84.7	-166.9
AChClO ₄ ⁱ	73.7	179.8
ACh,tg ^c	-155.6	79.8
ACh ^d	-179.2	76.0
ACh,tt ^{c,j}	180.0	180.0
ACh ^{d,j}	180.0	180.0
solution ^k	gauche	trans

^a Dihedral angles in deg. See structure 4 for numbering scheme.

^b ACh: acetylcholine. g: gauche. g': gauche'. t: trans. ^c This work. ^d Molecular mechanics structure, ref 38. ^e Crystal structure of acetylcholine bromide, ref 40. ^f Crystal structure of acetylcholine iodide, ref 41. ^g Crystal structure of acetylcholine tetraphenylborate, ref 42. ^h Crystal structure of acetylcholine chloride, ref 48. ⁱ Crystal structure of acetylcholine perchlorate, ref 49. ^j C_s symmetry. ^k References 39 and 43.

The magnitudes of the N₁C₅C₆O₇ and C₅C₆O₇C₈ torsional angles found from each of the above sources are collected in Table 2. Notice the reasonably wide range of gauche and trans dihedral angles allowed in the gas phase and in the crystals. The gauche dihedral angles of the isolated ACh ions tend to be smaller than those of the ACh ions in the crystalline compounds. However, only one of the calculated angles is outside the overall range seen experimentally.

Four of the five ACh rotamers are stabilized by internal C-H...O hydrogen bonding. The exception is the tt rotamer. C-H...O contacts are classified as hydrogen bonds if the H...O distance is ≤ 2.8 Å and the C-H...O bond angle is $\geq 90^\circ$. The 2.8 Å distance is the conservative cutoff used by Steiner and Saenger in the primary portion of their analysis of C-H...O hydrogen bonds in carbohydrate, amino acid, and metallo-organic crystals.¹⁰ A C-H...O contact limit of 3.2 Å was used for the remainder of their analysis. Our choices are also consistent with the ranges cited by Desiraju.⁴⁴ The intramolecular C-H...O hydrogen bonds exhibited by ACh are between the ester oxygen and a quaternary methyl hydrogen, between the carbonyl oxygen and a quaternary methyl hydrogen, and between the carbonyl oxygen and a CH₂ hydrogen. Similar types of C-H...O contacts have been cited for dimethoxyethane,²⁵ C_mH_{2m+1}OCH₂CH₂OH,¹⁴ carbohydrates,¹⁰ and nucleosides.⁴⁵

The gg' conformation of ACh has one three-center hydrogen bond in which a quaternary methyl hydrogen interacts with both the ester oxygen O₇ and the carbonyl oxygen O₉. (See structure 4 for the ACh numbering scheme.) Two other C-H...O=C interactions are also observed. Two of these hydrogen bonds, one C-H...O=C and one C-H...O-C, are repeated in the gg conformation. The gt and tg conformers contain only one C-H...O interaction, C-H...O-C and C-H...O=C, respectively.

D. Complexes of ACh with Water and Benzene: Computational. Possible interactions between water and ACh are (1) the ACh carbonyl oxygen binding to a water hydroxyl group O-H...O=C, (2) the water oxygen binding to one or more quaternary methyl or methylene groups C-H...O-H, (3) the

ACh ester oxygen binding to a water hydroxyl group C-O...H-O, and (4) the water oxygen binding to the acetoxy methyl group C-H...O-H. Possible interactions between an aromatic ring and ACh are (1) the π -ring binding to one or more quaternary methyl or methylene groups C-H... π and (2) the π -ring binding to the acetoxy methyl group C-H... π . The interactions involving a single methyl group and water or a single methyl group and an aromatic ring are of lower stability than the other interactions (this work and refs 9, 12, and 19–21), so the interactions involving the acetoxy methyl group will not be considered further in this article.

For four ACh conformations, when water forms a hydrogen bond with the carbonyl oxygen, it bridges between the oxygen and the choline moiety. That is, the water oxygen is the proton donor in an O-H...O=C hydrogen bond and the electron donor in two to four C-H...O hydrogen bonds. For example, for ACh,gt the water oxygen interacts with one methylene hydrogen and two methyl hydrogens, on different methyl groups. No such bridged structure was located for the gg' conformation of ACh, rather the ACh rotates to the gt conformation. When either water or benzene bind to the quaternary ammonium group, the ligand interacts with three hydrogens each from a different methyl group. Similar structures have been reported in earlier work on (CH₃)₄N⁺(H₂O) and (CH₃)₄N⁺(C₆H₆) complexes.^{9,20,31} In all of the arrangements examined for which the original water binding site was the ester oxygen, the water migrated to either the carbonyl oxygen or the quaternary ammonium function.

For the ACh(H₂O)₂ clusters, the second water molecule was bound to either the first water molecule or the quaternary ammonium group. Thus, four clusters were examined for each ACh conformation except the gg' conformation—one with a bridged C=O...H₂O...quaternary ammonium and a H₂O...H₂O interaction, one with a bridged C=O...H₂O...quaternary ammonium and a quaternary ammonium...H₂O interaction, one with a quaternary ammonium...H₂O...H₂O interaction, and one with two quaternary ammonium...H₂O interactions. Only the latter two configurations were considered for ACh,gg'. For the ACh(C₆H₆)₂ cluster ions, the second benzene was bound only to the quaternary ammonium moiety.

When ACh is in the gg, tg, or tt conformation and the second water molecule solvates a bridged water molecule, the second water interacts with only the first water. For the gt conformation of ACh, an additional structure was found in which a two-water bridge is formed with the oxygens from both water molecules acting as both electron and proton donors (C=O...H-O...H-O...H-C). A doubly bridged structure has also been identified as the most stable structure in complexes of two water molecules with diethers⁴⁶ and diketones.⁴⁷ In these cases, the protonated two-water molecule bridge can mediate proton transfer between the ether or ketone groups. The combined results indicate that doubly bridged geometries should routinely be explored for complexes between water and polyfunctional ions, as they may be a common feature in the hydration of polyfunctional ions. When the second water or benzene ligand interacts with the quaternary ammonium group, the interaction involves two or three hydrogens from different methyl or methylene groups.

To distinguish among the various ACh complexes, each ligand binding site has been assigned a one- or two-letter abbreviation. A one-water bridge has been designated br, and a two-water bridge has been designated br,br. Quaternary ammonium...ligand and H₂O...H₂O interactions have been

(44) Desiraju, G. R. *Acc. Chem. Res.* **1991**, *24*, 290–296.

(45) Jeffrey, G. A.; Saenger, W. *Hydrogen Bonding in Biological Structures*; Springer: Berlin, 1991.

(46) Meot-Ner (Mautner), M.; Sieck, L. W.; Scheiner, S.; Duan, X. *J. Am. Chem. Soc.* **1994**, *116*, 7848–7856.

(47) Meot-Ner (Mautner), M.; Scheiner, S. *J. Am. Chem. Soc.* In press.

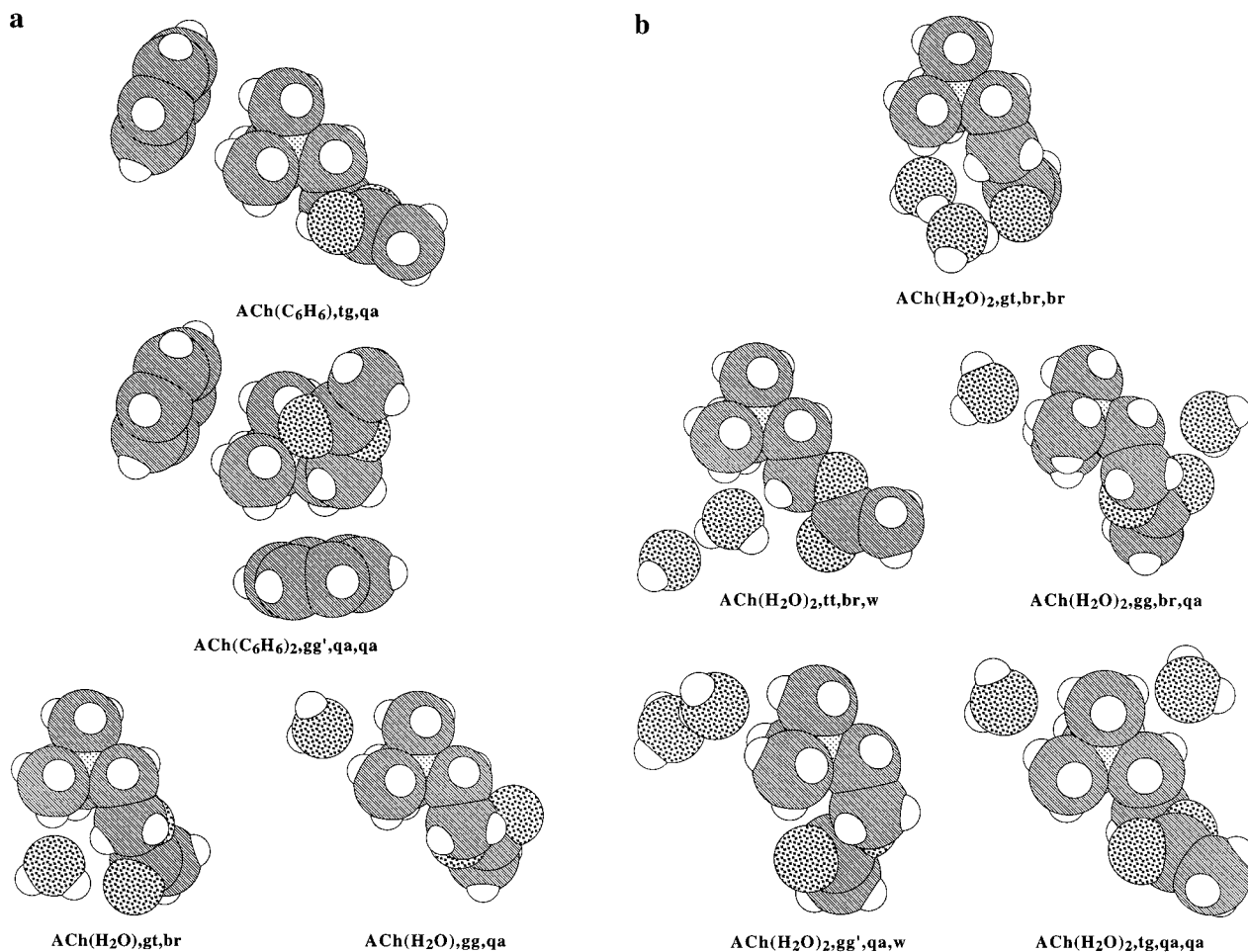


Figure 3. Space filling representations of ACh complexes. The degrees of grayness are: C > O > N > H.

designated qa and w, respectively. With these abbreviations in mind, the ACh(C₆H₆) complex with the tt rotamer of ACh would be represented as ACh(C₆H₆),tt,qa; the ACh(H₂O)₂ complex with the gt rotamer of ACh and a two-water bridge would be represented as ACh(H₂O)₂,gt,br,br; the ACh(H₂O)₂ complex with the gg' rotamer of ACh and a quaternary ammonium...H₂O...H₂O interaction would be represented as ACh(H₂O)₂,gg',qa,w. One complex of each type is displayed in Figure 3.

Solvating a particular ACh conformer does cause changes in the backbone dihedral angles, but the changes are generally less than 10°. Within a particular set of complexes the displacements are largest for the bridged structures. Nevertheless, the range of calculated dihedral angles is only 5° wider than the range observed experimentally.^{40–42,48,49} The data for all of the complexes have been tabulated and supplied as Supporting Information (Table S2).

To illustrate typical H...O distances and C–H...O angles, these geometrical parameters for the gt conformer of ACh and its complexes are presented in Table 3. The analogous parameters for the remaining ACh conformers are given in Table S3 in the Supporting Information. Bond angles smaller than 90° have been included in Table 3 to demonstrate the rearrangements that take place as ACh is solvated. When every system we examined is taken into account, the H...O bond distances range from 1.9 to 2.5 Å in the O–H...O hydrogen bonds and from 2.3 to 2.8 Å in the C–H...O hydrogen bonds. The hydrogen bond angles vary from 90 to 177°.

Although the internal C–H...O hydrogen bonds are shorter than the external C–H...O hydrogen bonds, the internal hydrogen bond angles are smaller, which is indicative of the

greater strain in these hydrogen bonds. Addition of a second water molecule often causes rearrangements that weaken the interactions involving the first water molecule. Compare, for example, the O₂₇...H distances in the ACh(H₂O),gt,qa,qa and ACh(H₂O),gt,qa clusters. Contrarily, for the complexes with a two-water bridge or a quaternary ammonium...H₂O...H₂O interaction, cooperative effects lead to a shortening of the C–H...O hydrogen bonds.

The distance between the nitrogen atom and the center of the benzene ring is 4.606 Å in ACh(C₆H₆),gt,qa. This N...φ distance is comparable to the value of 4.571 Å computed for (CH₃)₄N⁺(C₆H₆) at the HF/6-31G(d) level of theory.¹² The distances are 4.606 and 4.636 Å for the two benzenes in ACh-(C₆H₆)₂,gt,qa,qa.

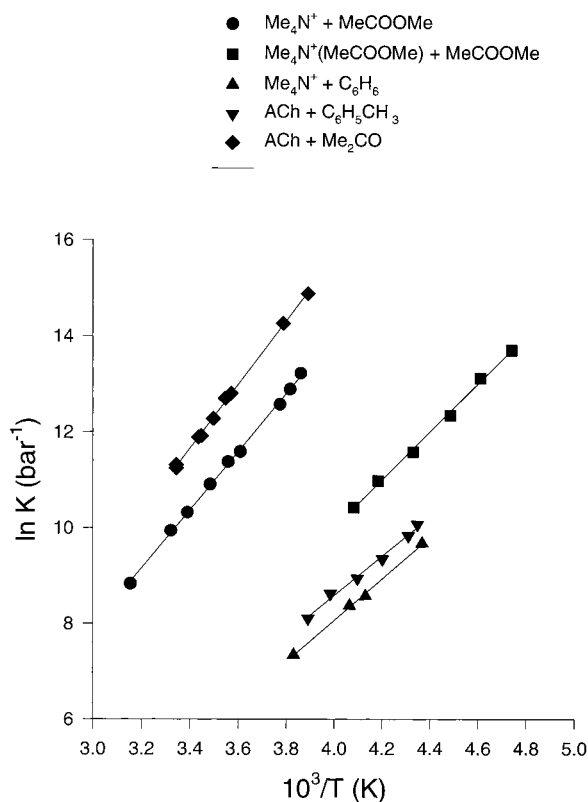
E. Thermochemistry of the Interactions of Quaternary Ions with Solvent and Ligand Molecules: Experimental.

Association equilibria 2 were measured as a function of temperature, and the van't Hoff plots are shown in Figure 4. The most serious limiting factor in these measurements is the low vapor pressure of CH₃CO₂CH₂CH₂N(CH₃)₂. As ACh is a methyl-blocked ion without strongly bonding protons, the binding energies are relatively small and require low temperatures for measurement purposes, at which CH₃CO₂CH₂CH₂N-(CH₃)₂ and some of the involatile ligands condense in the ion source. Therefore, the equilibrium could be observed at only one temperature in some cases, and the ΔG° was used with an estimated ΔS° value from similar reactions to calculate ΔH°. Since the ΔS° values are within ±17 J/(mol·K) (±4 cal/(mol·K)) of the estimated values for all the reactions measured, at 300 K this introduces an uncertainty of ±5 kJ/mol (±1.2 kcal/

Table 3. Hydrogen Bond Lengths and Angles of gt Complexes^{a,b}

complex	O ₇ ···H ₁₃	angle ^c	O ₉ ···H	angle ^c	O ₂₇ ···H	angle ^c	O ₃₀ ···H	angle ^c
ACh,gt	2.309	122.0	2.511 (22)	81.9				
ACh(H ₂ O),gt,br	2.639	98.5	2.407 (23)	90.3	2.519 (13)	152.0		
			2.175 (28)	138.9	2.408 (15)	154.1		
ACh(H ₂ O),gt,qa	2.328	120.6	2.519 (22)	81.7	2.444 (23)	141.6		
					2.724 (12)	144.4		
					2.466 (16)	153.0		
					2.491 (18)	149.8		
ACh(C ₆ H ₆),gt,qa	2.315	122.1	2.509 (22)	82.3				
ACh(H ₂ O) ₂ ,gt,br,br	2.484	105.5	2.085 (28)	141.6	2.641 (23)	146.8	2.412 (13)	151.2
					1.900 (31)	161.7	2.376 (15)	153.8
							2.729 (23)	122.3
ACh(H ₂ O) ₂ ,gt,br,w	2.606	99.6	2.315 (28)	132.9	2.409 (13)	151.8	1.927 (29)	176.8
					2.335 (15)	152.9		
					2.420 (23)	136.8		
ACh(H ₂ O) ₂ ,gt,br,qa	2.633	99.0	2.417 (23)	90.0	2.543 (13)	152.1	2.737 (14)	143.9
			2.170 (28)	139.5	2.437 (15)	154.5	2.518 (17)	151.0
					2.455 (23)	141.4	2.472 (21)	154.2
ACh(H ₂ O) ₂ ,gt,qa,w	2.334	120.5			2.605 (12)	142.5	1.924 (28)	169.3
					2.367 (16)	150.7		
					2.353 (18)	149.4		
ACh(H ₂ O) ₂ ,gt,qa,qa	2.333	121.8			2.520 (12)	151.8	2.529 (14)	149.8
					2.742 (16)	144.9	2.506 (21)	141.4
					2.498 (18)	152.8		
ACh(C ₆ H ₆) ₂ ,gt,qa,qa	2.325	122.2						

^a Bond lengths in Å, bond angles in deg. ^b Numbers in parentheses indicate hydrogen to which oxygen is hydrogen bonded. See structure 4 for ACh numbering scheme. Numbering scheme for water molecules: H₂₈O₂₇H₂₉ and H₃₁O₃₀H₃₂. ^c Angle O···H–X, where X = C or O.

**Figure 4.** Van't Hoff plots for association reactions as indicated.

mol) in the calculated ΔH° values. The results are summarized in Table 4, together with some previous results for the $(\text{CH}_3)_4\text{N}^+$ ion.⁹

First, we observe that the binding energies are relatively weak, in the range of 33–59 kJ/mol (8–14 kcal/mol) with most ligands. These values are consistent with those found for other C–H···O and C–H··· π complexes of blocked ions, and are significantly smaller than, for example, those found for (O–H···O)⁺-type ionic hydrogen-bonded dimers. The latter dimers are usually bonded by 60–125 kJ/mol (15–30 kcal/mol).

Comparing $(\text{CH}_3)_4\text{N}^+$ and $\text{CH}_3\text{CO}_2\text{CH}_2\text{CH}_2\text{N}(\text{CH}_3)_3^+$ complexes with several ligands shows that the binding energies are similar, although the latter complexes are systematically weaker by about 4 kJ/mol (1 kcal/mol). Although the difference is within the error limits, the systematic trend may reflect internal bonding in ACh as discussed below. In any event, the energies are similar enough so that $(\text{CH}_3)_4\text{N}^+$ may be used as a satisfactory model of $\text{CH}_3\text{CO}_2\text{CH}_2\text{CH}_2\text{N}(\text{CH}_3)_3^+$ in binding measurements.

In contrast to regular ionic hydrogen bonds, the attachment energy of a second ligand molecule is similar to that of the first ligand molecule. For regular ionic hydrogen bonds consecutive ligand binding energies usually decrease by a factor of about 0.3.¹⁶ The weak mutual effects may be due to the large size of the ion, which allows the ligand molecules to be well separated and to avoid mutual repulsion. Also, the charge on the large ion is already diffuse, so adding the first ligand molecule has a relatively small effect on the partial charge at the second binding site.

With the moderately polar ligands H₂O and CH₃OH, the binding energies are 33–42 kJ/mol (8–10 kcal/mol). Interestingly, the binding energies to the aromatic ligands C₆H₆ and C₆H₅CH₃ are similar. On the other hand, the polar organic ligands (CH₃)₂CO and CH₃CO₂CH₃ are more strongly bound by 13–21 kJ/mol (3–5 kcal/mol). The substituted aromatics 3-CH₃C₆H₄OH and C₆H₅OCH₃ have comparably stronger complexation energies, suggesting that they function as polar oxygen rather than aromatic ligands. Thus, tyrosine residues in the groove may also act as polar oxygen rather than aromatic ligands. A similar conclusion was reached by Pullman et al. based on their ab initio computations.³¹ Amide groups such as CH₃CON(CH₃)₂ or the peptide-like amino acid derivative CH₃-CONHCH₂CO₂CH₃ (i.e., methyl acetylglycinate) bind even more strongly, by up to 75–85 kJ/mol (18–20 kcal/mol).

These data suggest that aromatic residues such as phenylalanine may help to provide a stabilizing environment for ACh, which may be intermediate between the aqueous solvent and the ultimate binding site. The mechanistic implications are discussed below.

Table 4. Thermochemistry^a of Association Reactions of Ligand Molecules to Quaternary Ions

ligand	Me ₄ N ⁺			ACh		
	−ΔH°	−ΔS°	−ΔG°[T]	−ΔH°	−ΔS°	−ΔG°[T]
H ₂ O	37.7 ^c	90.0 ^c		33.5	92	12.1[229]
H ₂ O ^b	39.3 ^c	92 ^c	15.1[255] ^c			
CH ₃ OH	41.0 ^c	97.1 ^c				
CH ₃ OH ^b	38.5 ^c	100.4 ^c				
(CH ₃) ₂ CO	61.1 ^c	103.3 ^c		55.2(1.3)	90.8(4.6)	
(CH ₃) ₂ CO ^b	54.4 ^c	122.2 ^c				
CH ₃ CO ₂ CH ₃	50.6(1.3)	85.4(4.1)				
CH ₃ CO ₂ CH ₃ ^b	41.4(1.7)	83.3(8.4)				
3-CH ₃ C ₆ H ₄ OH				53.6	100	24.3[293]
C ₆ H ₅ OCH ₃				51.5	100	24.7[267]
CH ₃ CON(CH ₃) ₂	75.3 ^c	90.4 ^c				
CH ₃ CONHCH ₂ CO ₂ CH ₃	84.1 ^c	123.0 ^c				
(CH ₃ CO-Gly-OCH ₃)						
C ₆ H ₆	36.0(1.7)	77.0(6.7)				
C ₆ H ₅ CH ₃	39.7 ^c	84.9 ^c		33.9(2.9)	64.9(1.7)	

^a ΔH° and ΔG° in kJ/mol, ΔS° in J/(mol·K). Standard state bar⁻¹. Estimated values of ΔS° in italics used to derive ΔH° from ΔG° measured at temperature given. Uncertainty estimates, in parentheses, are based on the standard deviations of the slopes and intercepts of the van't Hoff plots, multiplied by a conventional coverage factor of 2. ^b Attachment thermochemistry of the second ligand molecule to ACh. ^c Reference 9.

Table 5. Calculated Relative Thermochemical Values for ACh(C₆H₆)_n, n = 0–2^{a,b}

species	ΔE _T	ΔH°	ΔS°	ΔG°
ACh,gg' ^c	(0.0)	(0.0)	(0.0)	1.7
ACh,gg' ^d	2.5	2.1	12.1	(0.0)
ACh,gt	6.3	5.4	12.6	3.3
ACh,tg	7.5	7.9	12.6	5.4
ACh,tt ^e	18.8	18.4	19.2	14.2
ACh(C ₆ H ₆),gg',qa ^f	3.3	3.8	(0.0)	5.9
ACh(C ₆ H ₆),gg,qa ^g	(0.0)	(0.0)	6.3	(0.0)
ACh(C ₆ H ₆),gt,qa	8.4	8.4	21.3	3.8
ACh(C ₆ H ₆),tg,qa	10.5	10.9	23.8	5.4
ACh(C ₆ H ₆),tt,qa	20.1	19.7	25.9	13.8
ACh(C ₆ H ₆) ₂ ,gg',qa,qa ^h	2.9	2.9	(0.0)	4.6
ACh(C ₆ H ₆) ₂ ,gg,qa,qa ⁱ	(0.0)	(0.0)	5.4	(0.0)
ACh(C ₆ H ₆) ₂ ,gt,qa,qa	7.1	6.7	17.2	3.3
ACh(C ₆ H ₆) ₂ ,tg,qa,qa	8.4	8.4	6.7	8.4
ACh(C ₆ H ₆) ₂ ,tt,qa,qa	17.2	16.7	16.7	13.4

^a ΔE_T, ΔH°, and ΔG° in kJ/mol, ΔS° in J/(mol·K). ^b MP2/6-31G(d)//HF/6-31G(d) data. ΔH°, ΔS°, and ΔG° at 298 K. ^c For ACh,gg', E_T = −479.785495 au, H = −479.519296 au, S = 0.000166804 au. ^d For ACh,gg, G = −479.569611 au. ^e C_s symmetry. ^f For ACh(C₆H₆),gg',qa, S = 0.000234643 au. ^g For ACh(C₆H₆),gg,qa, E_T = −711.258055 au, H = −710.877006 au, G = −710.947669 au. ^h For ACh(C₆H₆)₂,gg',qa,qa, S = 0.000306318 au. ⁱ For ACh(C₆H₆)₂,gg,qa,qa, E_T = −942.730059 au, H = −942.233938 au, G = −942.325888 au.

F. Relative Thermochemistry: Computational. Table 5 lists the MP2/6-31G(d)//HF/6-31G(d) relative total energies, enthalpies, entropies, and free energies of the various forms of ACh, ACh(C₆H₆), and ACh(C₆H₆)₂. The analogous data for ACh(H₂O) and ACh(H₂O)₂ are given in Table 6. The HF/6-31G(d)//HF/6-31G(d) relative thermochemical values have been provided as Supporting Information in Tables S4 and S5. Briefly, accounting for electron correlation does change the relative stabilities of the ACh conformers and of the water and benzene complexes derived from them.

For all of the ions investigated in this work, the relative total energies are essentially equivalent to the relative enthalpies. All complexes containing the gg' rotamer of ACh have a lower entropy, as do the more rigid complexes containing one or more bridged waters. The range of relative entropies tends to be wider than the range of relative enthalpies. This combination often leads to a different order for the relative enthalpies and free energies. The importance of entropy in determining relative stabilities has also been noted by Mhin et al.⁵⁰ in their study of the hexaquo-sodium(I) ion and by Tsuzuki et al.²⁵ in their study of 1,2-dimethoxyethane.

Table 6. Calculated Relative Thermochemical Values for ACh(H₂O)_n, n = 1, 2^{a,b}

species	ΔE _T	ΔH°	ΔS°	ΔG°
ACh(H ₂ O),gg',qa ^c	7.1	7.1	19.7	5.4
ACh(H ₂ O),gg,br	10.5	10.0	13.4	10.5
ACh(H ₂ O),gg,qa ^d	9.2	8.4	43.1	(0.0)
ACh(H ₂ O),gt,br ^e	(0.0)	(0.0)	(0.0)	4.2
ACh(H ₂ O),gt,qa	13.0	12.1	34.7	6.3
ACh(H ₂ O),tg,br	10.9	11.3	6.7	13.4
ACh(H ₂ O),tg,qa	13.8	13.8	38.1	7.1
ACh(H ₂ O),tt,br ^f	10.5	11.3	7.5	15.1
ACh(H ₂ O),tt,qa	23.4	23.0	38.1	15.9
ACh(H ₂ O) ₂ ,gg',qa,w	14.6	14.2	32.2	4.6
ACh(H ₂ O) ₂ ,gg',qa,qa	21.3	20.1	53.6	4.2
ACh(H ₂ O) ₂ ,gg,br,w	29.7	28.5	49.0	13.8
ACh(H ₂ O) ₂ ,gg,br,qa	21.8	20.1	45.6	6.3
ACh(H ₂ O) ₂ ,gg,qa,w	15.5	15.1	41.8	2.5
ACh(H ₂ O) ₂ ,gg,qa,qa	21.3	19.7	43.5	6.7
ACh(H ₂ O) ₂ ,gt,br,br ^g	(0.0)	(0.0)	(0.0)	(0.0)
ACh(H ₂ O) ₂ ,gt,br,w	13.1	11.8	31.2	2.5
ACh(H ₂ O) ₂ ,gt,br,qa	11.3	10.0	28.9	1.3
ACh(H ₂ O) ₂ ,gt,qa,w	19.7	18.8	46.0	5.0
ACh(H ₂ O) ₂ ,gt,qa,qa	25.1	23.4	66.9	3.3
ACh(H ₂ O) ₂ ,tg,br,w	25.1	24.7	43.9	11.3
ACh(H ₂ O) ₂ ,tg,br,qa	22.6	21.3	35.6	10.9
ACh(H ₂ O) ₂ ,tg,qa,w	20.9	20.5	45.2	7.1
ACh(H ₂ O) ₂ ,tg,qa,qa	27.6	26.4	68.6	5.9
ACh(H ₂ O) ₂ ,tt,br,w	23.4	23.4	34.7	13.0
ACh(H ₂ O) ₂ ,tt,br,qa	22.2	21.8	37.7	10.5
ACh(H ₂ O) ₂ ,tt,qa,w	28.9	28.0	45.2	14.6
ACh(H ₂ O) ₂ ,tt,qa,qa	36.0	34.3	68.6	13.8

^a ΔE_T, ΔH°, and ΔG° in kJ/mol, ΔS° in J/(mol·K). ^b MP2/6-31G(d)//HF/6-31G(d) data. ΔH°, ΔS°, and ΔG° at 298 K. ^c Bridged complex rotated to the gt conformation. ^d For ACh(H₂O),gg,qa, G = −555.767960 au. ^e For ACh(H₂O),gt,br, E_T = −555.004242 au, H = −555.708672 au, S = 0.000193385 au. ^f C_s symmetry. ^g For ACh(H₂O)₂,gt,br,br, E_T = −632.223964 au, H = −631.898631 au, S = 0.000217116 au, G = −631.963363 au.

(i) ACh and ACh(C₆H₆)_n, n = 1, 2. ACh,gg' has the largest number of intramolecular hydrogen bonds and the most negative total energy and enthalpy. ACh,tt has the least negative total energy and enthalpy. At the MP2/6-31G(d)//HF/6-31G(d) level of calculation, the internal solvation stabilizes the gg' conformer by about 19 kJ/mol (4.5 kcal/mol). The remaining three con-

(48) Herdtklotz, J. K.; Sass, R. L. *Biochem. Biophys. Res. Commun.* **1970**, *40*, 583–588.

(49) Mahajan, V.; Sass, R. L. *J. Cryst. Mol. Struct.* **1974**, *4*, 15–21.

(50) Mhin, B. J.; Kim, J.; Kim, K. S. *Chem. Phys. Lett.* **1993**, *216*, 305–308.

formers are stabilized by 10.5–17 kJ/mol (2.5–4 kcal/mol). Thus, the combined strength of the C–H···O interactions in any ACh rotamer is weaker than the 39 kJ/mol (9 kcal/mol) interaction in CH₃CO₂CH₂CH₂N(CH₃)₂H⁺ and the 50.6 kJ/mol (12.1 kcal/mol) interaction between CH₃CO₂CH₃ and (CH₃)₄N⁺. Neither result is surprising since CH₃CO₂CH₂CH₂N(CH₃)₂H⁺ contains a conventional (N–H···O)⁺ hydrogen bond and the (CH₃)₄N⁺(CH₃CO₂CH₃) complex will be less sterically constrained.

The enthalpy differences among the ACh rotamers are sufficiently small that the entropy differences lead to a reordering of the relative free energies compared to the relative enthalpies (Table 5). Although the most stable rotamer with respect to the free energy is ACh.gg, the results suggest that only the tt conformer is unlikely to contribute measurably to the gas-phase equilibrium population at 298 K ($\Delta G \geq 8.5$ kJ/mol (2 kcal/mol)). For the ACh(C₆H₆) and ACh(C₆H₆)₂ cluster ions, the ion with ACh in the gg conformation also has the most stable free energy. In each case, the relative free energies are reordered and compressed with respect to the relative enthalpies, but the most stable complex does not change. Again, the results suggest that for the tabulated ACh(C₆H₆)_n complexes, only ACh-(C₆H₆).tt,qa and ACh(C₆H₆)₂.tt,qa,qa are unlikely to contribute measurably to the gas-phase equilibrium populations at 298 K.

Since a number of ions within each of the three series in Table 5 have nearly equivalent stabilities, carrying out higher level calculations could reorder some of the free energies. However, it seems unreasonable that the results of those calculations will change the general conclusion that there is a mixture of conformers at equilibrium. Likewise, the inferences drawn from the thermochemical data on ACh(H₂O) and ACh-(H₂O)₂ are expected to be independent of calculational level (see below).

(ii) ACh(H₂O) and ACh(H₂O)₂. On the basis of the relative enthalpies of the nine ACh(H₂O) cluster ions, one would predict that only two or three structures would be present to any appreciable extent in the gas-phase equilibrium population of ACh(H₂O) at 298 K (Table 6). Those structures would be ACh-(H₂O).gt,br, ACh(H₂O).gg',qa, and ACh(H₂O).gg,qa. On the basis of the relative free energies, ACh(H₂O).gt,qa and ACh-(H₂O).tg,qa would be added to the list and the dominant form would change. The predominance of the qa complexes in the equilibrium mixture can be accounted for as follows. With the exception of the complex with the gg' conformation of ACh, the entropies of the complexes with a quaternary ammonium···water interaction are comparable in magnitude and are uniformly about 30 J/(mol·K) (7 cal/(mol·K)) larger than those for the corresponding bridged complexes. The difference in the predictions is even more pronounced for the ACh(H₂O)₂ cluster ions. Now the calculations suggest a conversion from one structure at equilibrium (ACh(H₂O)₂.gt,br,br) to twelve, again underscoring the importance of the entropy contribution to the free energy for the ACh systems. In this case, all but four of the structures have either a quaternary ammonium···water···water interaction or two quaternary ammonium···water interactions.

(iii) ACh Conformation in Aqueous Solution. The solution NMR studies of Culvenor and Ham³⁹ indicate that the gt form of ACh predominates in aqueous solution (Table 2). When water binds to the choline end of the molecule in the gas-phase clusters, the calculations suggest that the gg', gg, gt, and tg conformers of ACh(H₂O)_n, *n* = 1, 2, will contribute to the equilibrium mixtures (Table 6). When the acetylcholine–water interaction involves the carbonyl oxygen, the calculations suggest that the only competitive clusters are ACh(H₂O).gt,br

Table 7. Calculated Thermochemistry of Association Reactions ACh(B)_{*n*-1} + B → ACh(B)_{*n*}, *n* = 1, 2^a

ACh(B) _{<i>n</i>}	–Δ <i>H</i> ^o _{rx}	–Δ <i>S</i> ^o _{rx}	–Δ <i>G</i> ^o _{rx}
ACh(H ₂ O)	46.4	87.9	20.5
ACh(H ₂ O) ₂	54.4	125.9	17.2
ACh(C ₆ H ₆)	38.5	92.5	11.3
ACh(C ₆ H ₆) ₂	34.7	77.0	11.7

^a MP2/6-31G(d)//HF/6-31G(d) data. Δ*H*^o_{rx} and Δ*G*^o_{rx} in kJ/mol, Δ*S*^o_{rx} in J/(mol·K), *T* = 298 K.

or ACh(H₂O)₂.gt,br,br, ACh(H₂O)₂.gt,br,w, ACh(H₂O)₂.gt,br,-qa, and ACh(H₂O)₂.gg,br,qa. Overall, about 70% of the ACh-(H₂O)₂ cluster ions contain gt rotamers of ACh. Although the computational results are limited to only two water molecules, if the results can be extrapolated to the bulk solution they do provide a possible explanation for the predominance of the gt conformation of ACh in aqueous solution.

G. Thermochemistry of Association Reactions: Computational. The MP2/6-31G(d)//HF/6-31G(d) thermochemical values for reaction 2 are collected in Table 7. Recall that, rather than using weighted averages, the calculated enthalpies, entropies, and free energies of reaction have been estimated by assuming that the reactant and product ACh conformations are identical. Compared to the HF/6-31G(d)//HF/6-31G(d) data (Supporting Information, Table S6), the MP2/6-31G(d)//HF/6-31G(d) values are more negative.

The only cluster for which a direct comparison can be made between the computational and experimental results is ACh-(H₂O) (Tables 4 and 7). The magnitude of the calculated change in free energy for this cluster is too large, primarily because the magnitude of the change in enthalpy is too large. There are several possible reasons, in addition to the above assumption, for the overestimation of the theoretical enthalpy change. First, the value has not been corrected for BSSE. Second, the electrostatic component of the interaction energy tends to be overestimated with the 6-31G(d) basis set. The calculated reaction enthalpy for the formation of ACh(H₂O)₂ is likely to be overestimated for the same reasons. In contrast, Δ*H*^o_{rx} for ACh(C₆H₆) and ACh(C₆H₅CH₃) appear fortuitously to be quite reasonable when compared with the data for (CH₃)₄N⁺(C₆H₆) and (CH₃)₄N⁺(C₆H₅CH₃). Another point on which the two sets of results coincide is that the association energies of the first and second ligands are similar.

H. Internal vs External Solvation. We have reported previously that external solvation of protonated diamines can weaken and possibly displace internal solvation, and conversely, internal solvation can weaken the interaction with external solvents.³⁷ As we noted above, (CH₃)₄N⁺ bonds to neutrals somewhat more strongly than CH₃CO₂CH₂CH₂N(CH₃)₃⁺ does (Table 4), which may be due to intramolecular solvation in CH₃-CO₂CH₂CH₂N(CH₃)₃⁺. The observation that the binding energies to first and second ligand molecules are similar suggests, however, that mutual interactions between the internal and external solvent groups of the quaternary ammonium ion functionality are small. The difference of 4 kJ/mol (1 kcal/mol) found for the (CH₃)₄N⁺ and ACh binding energies is consistent with this conclusion.

With respect to the computations, the most extreme effect of external solvation on the internal solvation is the gg' → gt conformational change that occurs when water is bound to the carbonyl oxygen of ACh.gg'. In all other cases, although there are changes in the hydrogen bond lengths and angles, the intramolecular hydrogen bonding is maintained when water or benzene complexes with ACh. For example, solvation lengthens the O₇···H₁₃ distance and decreases the C₂–H₁₃···O₇ angle in

ACh_{gt} (Table 3). However, for some of the complexes, the weakening of the O₇···H₁₃ interaction is partially compensated for by a strengthening of the O₉···H₂₃ interaction. Another manifestation of the effect of external solvation on internal solvation is that the most stable ACh conformation is gg' in the isolated ion, whereas it is gg or gt in the cluster ions.

One way to determine how the intramolecular hydrogen bonding influences ACh···ligand interactions is to compare the relative enthalpies of the ions with the ACh_{tt} rotamer to those of the ions with the other rotamers (Tables 5 and 6). More specifically, the enthalpy of ACh_{tt} is 13.0 kJ/mol (3.1 kcal/mol) less stable than that of ACh_{gt}, whereas the enthalpy of ACh(H₂O)_{tt,qa} is 10.9 kJ/mol (2.6 kcal/mol) less stable than that of ACh(H₂O)_{gt,qa}. The difference in stability is 11.3 kJ/mol (2.7 kcal/mol) for ACh(C₆H₆)_{gt,qa} and ACh(C₆H₆)_{tt,qa}. Similar data are obtained for the other rotamers. This comparison indicates that if internal solvation affects the external solvation in these complexes, the effect is certainly small, in agreement with the above conclusion from the experimental data.

I. AChE–ACh Interactions. Acetylcholinesterase (AChE) is a serine esterase that hydrolyzes ACh at a rate close to the diffusion-controlled limit.^{51,52} The three-dimensional structures of *Torpedo californica* AChE and a complex between *Torpedo californica* AChE and the transition state analogue inhibitor m-(N,N,N-trimethylammonio)-2,2,2-trifluoroacetophenone (TMT-FA) have recently been solved by X-ray analysis.^{1,3} The crystallographic data combined with data from site-directed mutagenesis,^{53–55} kinetic and spectroscopic,^{52,56,57} chemical modification,⁵⁸ and molecular modeling^{1,55,59,60} studies have provided important insights into the high specific activity of AChE. One of the most intriguing features of the AChE structure is a narrow cavity, about 20 Å long, that penetrates nearly to the center of the enzyme and contains the active site.^{1,3} This cavity, designated the “aromatic gorge”, is lined with 14 highly conserved aromatic amino acids.⁶¹

The active site of AChE contains two primary subsites, the esteratic and anionic subsites.^{1,3,56} Two secondary subsites, the peripheral subsite and the acyl pocket, also have important roles in the catalytic mechanism.^{1,3,62} The esteratic subsite lies about 4 Å from the bottom of the cleft, contains the catalytic triad of Ser-200 (torpedo sequence numbering), His-440, and Glu-327, and is the site at which the acylation and deacylation steps of

catalysis occur. The oxyanion of the tetrahedral intermediate interacts with the NH groups of the residues constituting the oxyanion hole, namely Gly-118, Gly-119, and Ala-201.

The remaining three subsites are highly aromatic in amino acid content. The trimethylammonium group of the substrate fits snugly in a concave binding site formed by the Trp-84, Glu-199, and Phe-330 residues and three water molecules in the (misnamed) anionic subsite. Cationic ligands are selectively bound to this site. The acyl pocket comprises residues Gly-119, Trp-233, Phe-288, Phe-290, and Phe-331 and provides a tight fit for the acetoxymethyl group, thereby excluding ligands of larger size. Finally, the peripheral subsite is located at the opening of the aromatic gorge and residues Trp-279, Tyr-70, and Asp-72 are key components of this region. It has been proposed that the peripheral binding site serves to increase the concentration of ACh at the top of the cavity and, together with other aromatic amino acids lining the gorge, to provide an array of low-affinity binding sites to facilitate the passage of ACh to the active site.^{1,63–65} Another function of the aromatic residues may be to assist in desolvating ACh.⁷

The roles suggested above for the aromatic residues are supported by the relative binding energies found in our work. The binding energies of ACh and the model ion (CH₃)₄N⁺ to aromatic molecules are similar to those to a H₂O molecule, but weaker than those to polar organic molecules (Table 4). Although the measurements extend only to one or two solvent molecules and do not account for bulk effects, they suggest that aromatic residues can supply effective stabilization that allows entry from the aqueous solution yet avoids trapping of ACh by polar oxygen or amide groups of the protein. Thus, the measurements provide a quantitative basis for the proposed substrate binding to low-affinity sites followed by diffusion to the active site.^{1,63–65}

(i) Selectivity. The present results show that bond strengths of aromatic rings to quaternary ions, 33–42 kJ/mol (8–10 kcal/mol), are much weaker than those to Na⁺, 117.2 kJ/mol (28.0 kcal/mol),⁶⁶ or to K⁺, 80.3 kJ/mol (19.2 kcal/mol).⁶⁷ Selective binding to quaternary ions therefore requires other factors. Geometric constraints may supply one such factor, as the separation of aromatic residues in the wide channel^{1–3} may allow effective multiple interactions with the large quaternary groups, but not with alkali metal ions.

The selectivity may be enhanced by the ACh ion itself through a conformational change as the ACh leaves the aqueous environment. A conformational change may contribute to selectivity for ACh as it is of course not possible for alkali metal ions or for rigid quaternary ions. Our limited model suggests a number of ways in which a change in conformation and improved internal solvation can help stabilize ACh as it goes from the aqueous to the aromatic environment (Table 5). For example, assuming ACh is in the gt conformation in solution, if it desolvates to gt and rearranges to gg', an estimated 5 kJ/mol (1.2 kcal/mol) in enthalpy and 1.5 kJ/mol (0.4 kcal/mol) in free energy could be gained. If it rearranges to gg, an estimated 3 kJ/mol (0.7 kcal/mol) in both enthalpy and free

(51) Bazelyansky, M.; Robey, C.; Kirsch, J. F. *Biochemistry* **1986**, *25*, 125–130.

(52) Quinn, D. M. *Chem. Rev.* **1987**, *87*, 955–979.

(53) Shafferman, A.; Kronman, C.; Flashner, Y.; Leitner, M.; Grosfeld, H.; Ordentlich, A.; Gozes, Y.; Cohen, S.; Ariel, N.; Barak, D.; Harel, M.; Silman, I.; Sussman, J. L.; Velan, B. *J. Biol. Chem.* **1992**, *267*, 17640–17648.

(54) Radic, Z.; Gibney, G.; Kawamoto, S.; MacPhee-Quigley, K.; Bongiorno, C.; Taylor, P. *Biochemistry* **1992**, *31*, 9760–9767.

(55) Ordentlich, A.; Barak, D.; Kronman, C.; Flashner, Y.; Leitner, M.; Segall, Y.; Ariel, N.; Cohen, S.; Velan, B.; Shafferman, A. *J. Biol. Chem.* **1993**, *268*, 17083–17095.

(56) Froede, H. C.; Wilson, I. B. In *The Enzymes*, 3rd ed.; Boyer, P. D., Ed.; Academic Press: New York, 1971; Vol. 5, pp 87–114.

(57) Eastman, J.; Wilson, E. J.; Cerveñansky, C.; Rosenberry, T. L. *J. Biol. Chem.* **1995**, *270*, 19694–19701.

(58) Harel, M.; Schalk, I.; Ehret-Sabatier, L.; Bouet, F.; Goeldner, M.; Hirth, C.; Axelsen, P. H.; Silman, I.; Sussman, J. L. *Proc. Natl. Acad. Sci. U.S.A.* **1993**, *90*, 9031–9035.

(59) Hosea, N. A.; Radic, Z.; Tsigelny, I.; Berman, H. A.; Quinn, D. M.; Taylor, P. *Biochemistry* **1996**, *35*, 10995–11004.

(60) Antosiewicz, J.; Wlodek, S. T.; McCammon, J. A. *Biopolymers* **1996**, *39*, 85–94.

(61) Gentry, M. K.; Doctor, B. P. In *Cholinesterases: Structure, Function, Mechanism, Genetics, and Cell Biology*; Massoulié, J.; Bacou, F.; Barnard, E.; Chatonnet, A.; Doctor, B. P.; Quinn, D. M., Eds.; American Chemical Society: Washington, DC, 1991; pp 394–398.

(62) Taylor, P.; Lappi, S. *Biochemistry* **1975**, *14*, 1989–1997.

(63) Adam, G.; Delbruck, M. In *Structural Chemistry in Molecular Biology*; Rich, A., Davidson, N., Eds.; Freeman: San Francisco, 1968; pp 198–215.

(64) Eigen, M. In *Quantum Statistical Mechanics in the Natural Sciences*; Mintz, S. L., Widinger, S. M., Eds.; Plenum: New York, 1974; pp 37–61.

(65) Pang, Y.-P.; Quiram, P.; Jelacic, T.; Hong, F.; Brimijoin, S. *J. Biol. Chem.* **1996**, *271*, 23646–23649.

(66) Guo, B. C.; Purnell, J. W.; Castleman, A. W., Jr. *Chem. Phys. Lett.* **1990**, *168*, 155–160.

(67) Sunner, J.; Nishizawa, K.; Kebarle, P. *J. Phys. Chem.* **1981**, *85*, 1814–1820.

energy could be gained. Conversion from ACh(C₆H₆)₂,gt,qa,qa to ACh(C₆H₆)₂,gg,qa,qa could lead to an estimated 6.5 kJ/mol (1.6 kcal/mol) gain in enthalpy and 3 kJ/mol (0.7 kcal/mol) gain in free energy. Another favorable factor is the large increase in entropy that could be obtained by releasing ACh from a doubly bridged configuration (Table 6).

(ii) Transition State Stabilization. Modeling studies,¹ structure–activity studies,⁶⁸ and the conformation of TMTFA in the trifluoroketone transition state analogue complex³ suggest that ACh has the tt conformation in the acylation transition state. Rotation of ACh to the tt conformation may be facilitated by the aromatic residues in the cleft (Tables 5 and 6). The enthalpy of the most stable ACh(H₂O)₂ complex, ACh(H₂O)₂,gt,br,br, lies some 22 kJ/mol (5.5 kcal/mol) below that of the most stable tt complex, ACh(H₂O)₂,tt,br,qa, whereas the enthalpy of the most stable ACh(C₆H₆)₂ complex, ACh(C₆H₆)₂,gg,qa,qa, lies some 17 kJ/mol (4.1 kcal/mol) below that of ACh(C₆H₆)₂,tt,qa,qa. It seems, therefore, that the aromatic environment may decrease the energy barrier to formation of the tt rotamer compared with aqueous solution. The data in Tables 5 and 6 also indicate that when H₂O or C₆H₆ binds to the choline end of the ACh ion, the relative enthalpies and free energies of the complexes generally closely parallel those of the isolated ACh rotamers. In particular, $H^\circ(\text{ACh,tt}) - H^\circ(\text{ACh,gg})$, $H^\circ(\text{ACh}(\text{C}_6\text{H}_6)_2, \text{tt,qa}) - H^\circ(\text{ACh}(\text{C}_6\text{H}_6)_2, \text{gg,qa})$, and $H^\circ(\text{ACh}(\text{H}_2\text{O})_2, \text{tt,qa}) - H^\circ(\text{ACh}(\text{H}_2\text{O})_2, \text{gg,qa})$ are 16.3 (3.9 kcal/mol), 19.7 (4.7 kcal/mol), and 14.6 kJ/mol (3.5 kcal/mol), respectively. The corresponding values for the free energies are 14.2 (3.4 kcal/mol), 13.8 (3.3 kcal/mol), and 15.9 kJ/mol (3.8 kcal/mol), respectively. Thus, conversion of ACh to the rare tt conformation would appear to have little effect on the enthalpies and free energies of complexation provided by the quaternary ammonium moiety/aromatic residue and quaternary ammonium moiety/water molecule interactions.

Harel et al.³ utilized data from site-directed mutagenesis experiments^{53–55} to estimate the contributions various enzyme–ligand interactions make to the free energy of stabilization of the acylation transition state. The net stabilization was obtained by assuming that the individual contributions are additive. That assumption is supported by our result that there is little difference in the binding energies of ACh to first and second ligand molecules (Tables 4 and 7). In their computer simulation studies of the acylation step of ACh hydrolysis, Fuxreiter and Warshel²² focused on the overall catalytic effect of the enzyme by comparing the energy barriers associated with the acylation step and the reference reaction in water. However, they also estimated the effect of individual interactions. Both groups assign 17–21 kJ/mol (4–5 kcal/mol) of transition state stabilization to the interaction between the quaternary ammonium moiety and Trp-84. Moreover, the simulation studies indicate that the ground state and transition state are stabilized by about the same amount. The magnitudes of the ground state and transition state binding energies are consistent with the data in Table 4. As Fuxreiter and Warshel point out,²² their results are also consistent with the observation⁵⁵ that mutation of Trp-84 reduces $k_{\text{cat}}/K_{\text{M}}$ by $\sim 10^3$ but changes k_{cat} very little.

With respect to stabilization of the oxyanion in the transition state, our previous cluster ion models of similar systems, i.e., serine proteases, showed that hydrogen bonding of the oxyanion to backbone amide hydrogens can stabilize the oxyanion by about 145 kJ/mol (35 kcal/mol).¹⁵ In this manner, gas-phase cluster models and the present calculations show that uncon-

ventional C–H $\cdots\pi$ bonds at the cationic site and strong (N–H \cdots O)[–] hydrogen bonds at the anionic site can stabilize the transition state in AChE by as much as 165 kJ/mol (40 kcal/mol), although in the condensed phase these effects may be reduced by the polar medium. The cluster models therefore support and help to quantify the conclusion of Fuxreiter and Warshel²² that “dipolar residues [the main chain amide NH groups of Gly-118, Gly-119 and Ala-201] help in direct stabilization of the transition state”. Harel et al.³ also noted the importance of the N–H \cdots oxyanion hydrogen bonds in stabilizing the transition state and assigned, by default, a total of 21–29 kJ/mol (5–7 kcal/mol) of transition state binding energy to these interactions.

J. Future Work. The present model could be improved by examining the solvation of ACh by various combinations of water and arene molecules. Consequently, ab initio calculations on mixed water/benzene cluster ions ACh(H₂O)_m(C₆H₆)_n are currently underway in our laboratory. We would also suggest that the corresponding experimental measurements might be possible through the use of tandem mass spectrometry, where the ACh ion could be generated externally to the ion source. It would also be interesting to see whether such methods could be applied to other ammonium or quaternary transmitter ions and other biological ions from involatile precursors.

Summary

In summary the following points have been made.

(1) The binding energies of the quaternary ions (CH₃)₄N⁺ and acetylcholine (ACh) to C₆H₆ and C₆H₅CH₃ are similar to those to H₂O (33–42 kJ/mol (8–10 kcal/mol)), but are weaker than those to polar organic ligands such as (CH₃)₂CO and CH₃CO₂CH₃ (50–63 kJ/mol (12–15 kcal/mol)) and to amides (up to 84 kJ/mol (20 kcal/mol)). Thus, the aromatic residues that line the groove leading to the ACh receptor site may provide effective stabilization that allows entry from the aqueous environment, yet avoids trapping of ACh by polar protein groups.

(2) Four of the five ACh rotamers identified computationally are stabilized by internal C–H \cdots O hydrogen bonds involving the quaternary ammonium group, which is supported by the thermochemistry of the protonated analogue, CH₃CO₂CH₂CH₂N(CH₃)₂H⁺, and by the measured substantial bonding energy of 50 kJ/mol between models of the ACh end groups, (CH₃)₄N⁺ and CH₃CO₂CH₃.

(3) Each conformer can form a number of stable complexes with water or benzene through O–H \cdots O=C, O–H \cdots O–C, O–H \cdots O–H, C–H \cdots O–H, and C–H $\cdots\pi$ interactions. The calculated trends in relative enthalpies often differ from the trends in relative free energies, indicating the importance of the entropy contribution to the stabilities of the ACh systems.

(4) The most stable hydrated structure has a bridge of two water molecules between the quaternary moiety and the carbonyl oxygen of ACh. About 70% of the ACh(H₂O)₂ cluster ions contain gt rotamers of ACh, which provides a possible explanation for the predominance of the gt conformation of ACh in aqueous solution.

(5) Strengthening intramolecular interactions, through conformational changes when ACh becomes partially desolvated upon entry into the channel, may compensate in part for the loss of bulk solvation. This intramolecular conformational assistance may also increase selectivity for ACh compared with rigid ions.

(6) The aromatic environment may play a further role when formation of the active all-trans ACh rotamer is required. The

(68) Schowen, K. B.; Smisman, E. E.; Stephen, W. F., Jr. *J. Med. Chem.* **1975**, *18*, 292–300.

calculations show that the aromatic environment may decrease the energy barrier to the formation of this active rotamer, which is required at the receptor site.

Supporting Information Available: A table of equilibrium structures for ACh. Tables of backbone dihedral angles, hydrogen bond parameters and relative thermochemical values for ACh and the complexes. A table of calculated thermochem-

istry for the association reactions $\text{ACh(B)}_{n-1} + \text{B} \rightarrow \text{ACh(B)}_n$, $n = 1, 2$. All geometrical parameters were obtained with the HF/6-31G(d) basis set, and all single-point energies were obtained at the HF/6-31G(d)//HF/6-31G(d) level of calculation (PDF). This material is available free of charge via the Internet at <http://pubs.acs.org>.

JA982549S